Flow between a plane wall and an oscillating circular cylinder in still water at low KC and Reynolds number

J.G. Tom[1] and S. Draper[1,2]

[1]Centre for Offshore Foundation Systems
University of Western Australia, Perth, Western Australia 6009, Australia

[2]School of Civil, Environmental and Mining Engineering
University of Western Australia, Perth, Western Australia 6009, Australia

Abstract

The flow field that results between a plane wall and a normally oscillating cylinder is explored through a series of particle image velocimetry (PIV) experiments. Sinusoidal cylinder motion is considered for Keulegan Carpenter (KC) numbers between 1 – 10 and Reynolds numbers (Re) less than 5000 (holding β=Re/KC constant). A constant minimum gap ratio between the cylinder and wall equal to 0.125 is adopted for all experiments. For sufficiently small KC and Re, the measured flow velocities beneath the cylinder show good comparison with both analytical predictions based on continuity arguments and on potential flow theory. At larger KC number asymmetry results, which is not captured in the analytical predictions. Over the full parameter space the results are used to explore the relationship between the motion of the cylinder and the flow velocity near the wall. It is believed that this relationship is important for quantifying the sediment transport beneath offshore infrastructure such as riser pipelines and mooring line chains, which oscillate normal to the seabed.

Introduction

Oscillation of circular cylinders normal to a plane wall has engineering applications relating to: the behaviour of pipeline risers near the touchdown zone [1]; the vibration of seabed pipelines; mooring line behaviour; and, in the medical industry, microcantilevers [2]. The fluid flow characteristics around oscillating cylinders without the presence of a wall have been extensively studied in recent decades [3, 4, 5]. However, little work has investigated the effect of a nearby boundary on the hydrodynamics of a normally oscillating cylinder, other than work focussing on vortex induced vibrations in the presence of external hydrodynamic flows.

The presence of a wall is expected to change the flow patterns around oscillating objects in at least two ways:

1. Lateral 'pumping' of fluid will occur beneath the object as it approaches the wall and moves away from the wall, and
2. The presence of the wall may affect vortex shedding caused by oscillation.

These effects are explored in this paper for a cylinder oscillating normal to a wall with position (see also Figure 1)

$$y(t) = H_{min} + A - A\cos\left(\frac{2\pi t}{T}\right) \qquad (1)$$

where H_{min} is the minimum distance to the wall, A is the amplitude of the motion and T is the period of the motion. The cylinder is closest to the wall when t/T =0, 1.
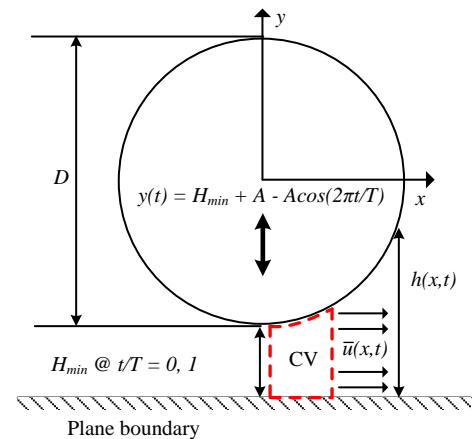

Figure 1. Problem definition.

Application to Steel Catenary Risers

A motivation for the work in this paper is to study the flow velocity near the wall so as to better understand sediment transport and 'trenching' that is often observed at the touchdown zone of Steel Catenary Risers (SCRs) on mobile seabeds [1]. Predicting the occurrence of sediment transport and the rate (and ultimate depth) of these trenches requires predictions of the velocities induced in the near seabed environment by oscillating objects.

The motions of an SCR at any particular location along its length varies depending on vessel motions, location, metocean conditions and the proximity to the touchdown zone. However, the amplitude of motion close to the touchdown zone, which is the focus of this work, is normally on the order of 1-2 diameters. Similar motions are also typical of pipelines during installation in normal operating conditions [6]. Therefore, motions with Keulegan Carpenter (KC) number in the range $1 < KC < 12$ are relevant to oscillating risers or pipelines near the seabed, with

$$KC = 2\pi A/D \qquad (2)$$

where D is the object diameter (see Figure 1).

This paper explores the flow induced by a circular cylinder oscillating normal to a plane boundary such that $KC < 10$. This investigation has been undertaken by performing experiments in which a cylinder is oscillated sinusoidally according to (1) in otherwise still water. The resulting flow field is captured using particle image velocimetry (PIV). In each experiment the Reynolds numbers (Re) was held at less than 5000, corresponding to a constant β (=Re/KC) of 500. The Reynolds is given by

$$Re = U_m D/\nu \qquad (3)$$

where U_m represents the peak velocity (=$2\pi A/T$) and ν the fluid viscosity.

The primary aims of the experiments were to: (a) investigate near bed flow field in the range $1 < KC < 10$; and (b) to demonstrate the applicability of various theoretical solutions to predict flow field beneath the cylinder at different KC. To explore the flow beneath the cylinder, both the lateral velocity (parallel to the wall) and the Eulerian particle excursion in the same direction (experienced over the course of a cycle at a given point beneath the cylinder) are analysed, where the latter is made non-dimensional so that

$$KC^+ = d^+/D \qquad (4)$$

where d^+ is the maximum Eulerian displacement during a cycle. This latter metric, which quantifies the integrated velocity over a half cycle, may also be relevant to the net displacement of sediment from beneath an SCR and, in turn, the dimensions of a trench which might form on a mobile seabed.

Theoretical solutions for the velocity near the wall

At small KC number potential flow may be used to predict the flow velocity beneath the riser, since flow separation is expected to be limited. Carpenter [7] presented a potential flow solution for two cylinders moving in an infinite ideal fluid, represented as an infinite series of image doublets, i.e. two cylinders with the same diameter moving in line with each other is analogous to a single cylinder moving normal to a smooth wall. The complete solution is not reproduced here for brevity; however results computed based on the Carpenter [7] solution are presented later in this paper. For these solutions we found that three image doublets was sufficient to achieve reasonable convergence (where the minimum gap distance was 12.5% of the pipeline diameter). More doublets are required for small gaps.

An even simpler approximation to estimate the lateral velocity beneath the cylinder can be found from continuity arguments. Taking a Control Volume (CV) beneath the cylinder as a function of distance from the centreline and time (dashed line Figure 1), the incremental change in volume is equal to the mean flow rate leaving the control volume. Utilising symmetry and assuming sinusoidal motion, it follows that:

$$\bar{u}(x,t) = xU_m sin\left(\frac{2\pi t}{T}\right) \times$$

$$\left(H_{min} + A - Acos\left(\frac{2\pi t}{T}\right) + \frac{D}{2} - \left(\left(\frac{D}{2}\right)^2 - x^2\right)^{1/2}\right)^{-1} \qquad (5)$$

where $\bar{u}(x,t)$ is the horizontal velocity averaged over the height $h(x,t)$ bounded between the wall and the cylinder; i.e.

$$\bar{u}(x,t) = \frac{1}{h(x,t)}\int_0^{h(x,t)} u(x,y,t)dy \qquad (6)$$

Equation (5) is applicable provided $|x| < D/2$. As expected the solution from (5) agrees with the mean horizontal velocity beneath the cylinder derived from potential flow. However, at any point beneath the cylinder the two solutions may differ because the velocity obtained from continuity represents a mean velocity.

The theoretical solutions due to continuity and potential flow may approximate the flow when vortex shedding is minimal. For a free-field cylinder, Williamson [3] described ranges of KC where various vortex shedding regimes occur. Below KC 4, the vortices form symmetrically on the trailing side of the cylinder but do not shed during half-cycles. It is therefore expected that the theoretical solutions should provide a reasonable approximation in this range of motion, before vortex shedding becomes prominent.

Experimental setup

Experiments were conducted in a section of a recirculating wave flume at the University of Western Australia. The flume has a width of 0.4 m and height of 0.5 m. Acrylic cylinders with a diameter of either 25 or 40 mm were oscillated using a belt-driven linear actuator. The cylinder was attached vertically to the actuator and oscillated horizontally along the flume. A 20 mm thick Perspex wall was positioned across the flume and clamped in place during wall tests. A 5-Watt continuous wave Argo-ion laser was used for illumination, producing an approximately 1-2 mm thick light sheet. Synthetic polycrystalline particles with median particle diameter of approximately 1 to 5 μm were used. Images were captured using a high speed Photron (FASTCAM SA3), with typical resolution of 768 pixels by 512 pixels at a frame rate of 500 frames/s and an exposure time of 1/1000 s. Images were recorded to cover a minimum of 10 cycles for each test combination and the results are presented as ensemble-averaged at various phases.

PIV analyses were conducted using the freely available software GeoPIV-RG [8], which incorporates first-order subset deformation shape functions and inverse compositional Gauss-Newton sub-pixel interpolation to examine cross-correlation of image pairs. For these analyses, subsequent image pairs (i.e. 1/500 s time difference) were analysed with 32 px by 32 px interrogation patches with 50 % overlap. This corresponds to a patch size of about 3.5 mm with the adopted field of field, which is sufficient to describe the overall flow behaviour and velocity characteristics but is not sufficient to, for instance, extract detailed information regarding boundary layers or turbulence.

**Experimental results**

Near wall flow

The experimental results are first assessed focusing on the behaviour near the wall to investigate the lateral 'pumping' velocities beneath the cylinder. Figure 2 shows velocity vectors for KC 4 (2a, 2b) and KC 10 (2c, 2d) at two different phases during the cycle. Results for KC 4 show that the flow responds to the direction of the cylinder motion symmetrically about the centre of the cylinder. For KC 10, the flow direction is clearly asymmetric, especially at $t/T = 0.1$. Figure 2c also shows evidence of the formation of a trailing vortex as the cylinder moves away from the wall.
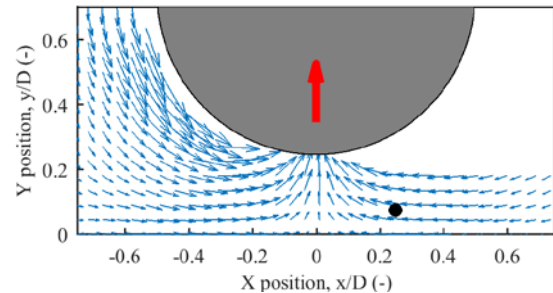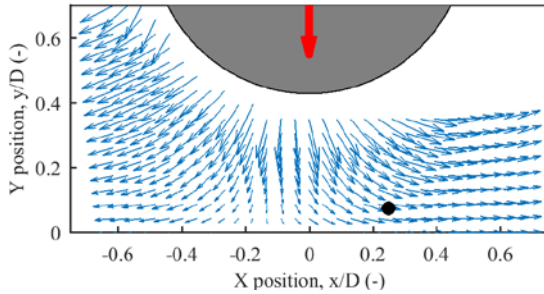

(a) KC 4, $t/T = 0.1$
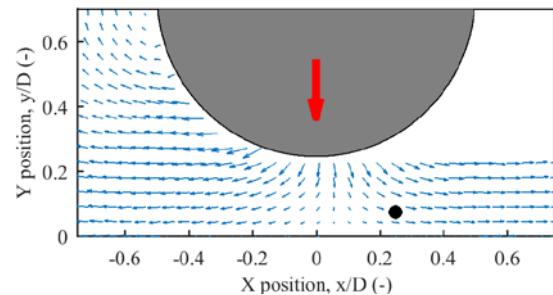

(b) KC 4, $t/T = 0.9$
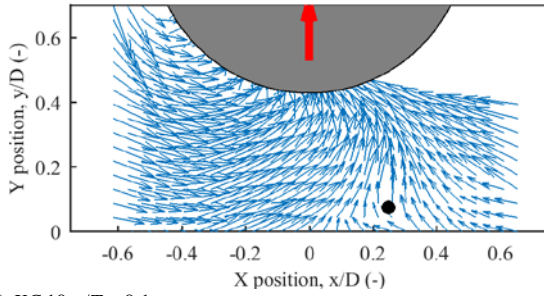
(c) KC 10, t/T = 0.1

(d) KC 10, t/T = 0.9

Figure 2. Example fluid velocity vectors: Vector magnitudes in units of *mm/s* all scaled by 1/500. Location of velocity comparison noted in black – x/D = 0.25; y/D = 0.075.

Figure 3 shows the phase-averaged lateral velocity obtained from PIV at a point located at x/D = 0.25 and y/D = 0.075 (as identified on Figure 2) for KC 4 and 10 as a function of cylinder velocity (i.e. at different points in the cycle). The predicted velocities based on potential flow and continuity are also presented. All sets of results generally show a similar asymmetric lemniscate shape. The PIV results for KC 4 suggest that the velocity is increased compared to the potential flow predictions when the cylinder is furthest away from the wall. This is believed to be caused by the formation of circulation cells, which will be explored in detail in the next section. Otherwise, the results for KC 4 generally show the measured flow velocity agrees reasonably well with the potential flow predictions and the solution based on continuity, particularly as the cylinder approaches the bed.

For KC 10 a similar figure eight shape is evident but the flow is significantly stronger in the positive direction than predicted by potential flow or continuity. This behaviour is caused by asymmetry in the overall flow field where the vortex formed just before the end of the cycle continues in the previous direction of motion and wraps around the temporarily halted cylinder. For a free cylinder, the vortices are able to convect away from the cylinder [3]; however, the presence of the wall prevents this and instead concentrates flow in the gap beneath the cylinder, causing a 'slingshot' amplification effect.

The results in Figure 3 may also be assessed in terms of maximum Eulerian particle excursion over the course of a cycle (d+), which better quantifies the integrated magnitude and direction of the flow. A 10th order polynomial was fit to the PIV velocities (measured at the previously specified point) in time – horizontal velocity space. The integration of this polynomial over the time when the velocity is positive outward corresponds to the maximum Eulerian excursion over one (ensemble-averaged) cycle.
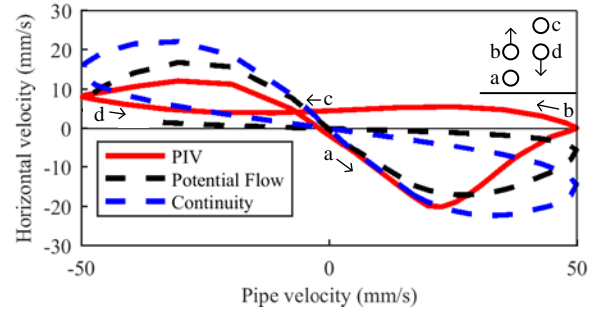
(a) KC = 4
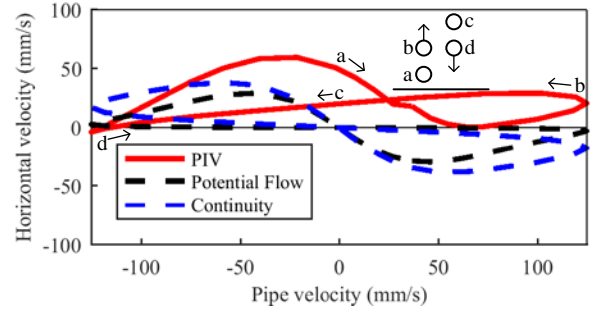
(b) KC = 10

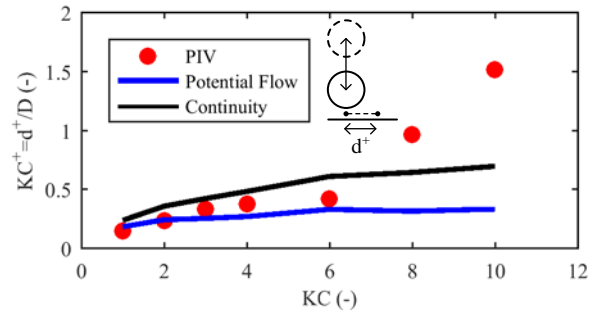Figure 3. Measured fluid velocity at x/D = 0.25, y/D = 0.075.

Figure 4. Eulerian fluid particle displacement at x/D = 0.25, y/D = 0.075 normalised by cylinder diameter.

The results of the Eulerian excursions are shown on Figure 4 for KC 4 and 10, as well as other values of KC less than 10, normalised by the cylinder diameter. At low KC the excursion KC^+ is relatively small and gradually increases with increasing KC up to 6. Above KC 6 there is an obvious increase in the excursion and divergence from theoretical predictions with increasing KC, which is consistent with the previous observations based on Figure 3b.

Overall flow

Trends in the overall flow behaviour can be observed on Figure 5, which present velocity vector results: the LHS of each subfigure shows PIV results and the RHS shows the corresponding potential flow result.

At low KC the pumping action beneath the cylinder was evident from Figure 2a and 2b. Figure 3a also demonstrates this to be consistent with potential flow theory, particularly for motion towards the wall. However, this does not explain the outward bias of the flow when the cylinder is away from the wall. Figure 5a shows ensemble-averaged vectors for KC = 4 at t/T = 0.55. The presence of an attached trailing vortex is evident but importantly the remnants of the previous half-cycle trailing vortices are seen near the wall. These remnant vortex pairs appear to contribute to circulation cells with the same vorticity direction as the previous trailing vortices, increasing the outward velocity near the wall. The wall prevents these vortex pairs from moving away, which would normally occur for a free-field cylinder. This motion is obviously not captured by potential flow, leading to the negative velocity bias in Figure 3a.

Velocity vectors for *KC* 10 are shown on Figure 5b and 5c for *t/T* = 0.9 and 0.05, respectively. In both of these figures, a shed vortex is seen above the cylinder, which progresses in the negative direction between 5b and 5c. The approximately transverse vortex street appears to remain in the presence of the wall. The street may not be interfered with significantly because the vast majority of vortex formation physical occurs between the extremes of the oscillation.

From Figure 5b, the wake behind the cylinder is evident from the nascent second vortex forming in the half cycle. Beneath the cylinder the flow appears relatively similar to the potential flow at this stage. However, after the end of the cycle and upon resumption of motion, the preceding wake appears to accelerate around the cylinder and the velocity becomes localised beneath the cylinder, as shown on Figure 5c. This creates the magnified velocity and asymmetry shown on Figures 3 and 4.
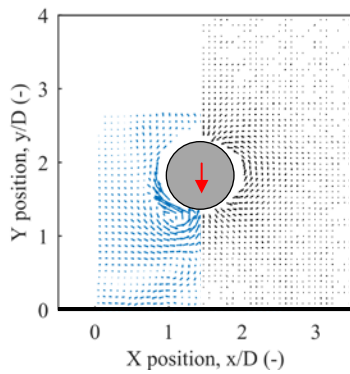
(a) *KC* 4, *t/T* =0.55
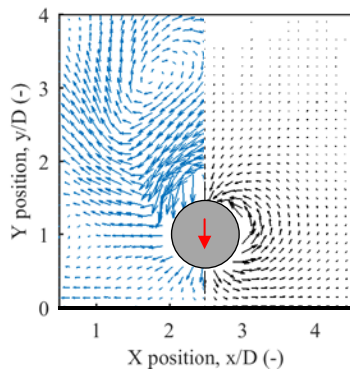
(b) *KC* 10, *t/T* = 0.9
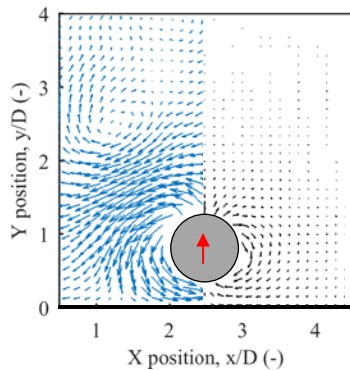
(c) *KC* 10, *t/T* =0.05

Figure 5. Comparison of horizontal velocities with potential flow: LHS – Experiment; RHS – Potential Flow

Conclusions

In this paper the flow features around and beneath a cylinder oscillating perpendicular to a wall have been investigated through PIV analyses. Experiments were conducted at low *KC* (< 10) and *Re* (< 5000).

Results indicate that for *KC* < ~4 symmetric 'pumping' occurs as the cylinder approaches and moves away from the wall. The magnitude and time variation of lateral velocities associated with pumping are reasonably predicted using potential flow theory and continuity arguments. Potential flow diverges from measured velocities near the wall when the cylinder is far from the wall due to counter-rotating circulation cells fed by released vortices following reversal at the end of cycles.

For *KC* > ~4 vortex shedding starts to dominate the velocity near the wall over the majority of the oscillation cycle. The lateral velocities near the wall become directionally asymmetric and their magnitude significantly amplified compared to predictions based on potential flow or continuity (for a symmetric flow) due to the impact of the trailing wake formed on the previous half cycle as the cylinder approaches the wall.

These findings suggest that potential flow and continuity arguments may be appropriate for predicting fluid motions and sediment transport beneath oscillating objects for low *KC* motions but not motions of higher amplitude. Example calculated Eulerian particle excursions are provided, which provide insight into the flows at higher *KC*.

References

[1] Bridge, C.D. & Howells, H.A., Observations and Modeling of Steel Catenary Riser Trenches, in *Proc. Int. Offshore & Polar Eng. Conf.*, Lisbon, 2007, 803-813.

[2] Clarke, R.J., Cox, S.M., Williams, P.M., & Jensen, O.E., The drag on a microcantilever oscillating near a wall, *Jour. Fluid Mech.*, **545**, 2005, 397-426.

[3] Williamson, C.H.K., Sinusoidal flow relative to circular cylinders, *Jour. Fluid Mech.*, **155**, 1985, 141-174.

[4] Sumer, B.M. & Fredsøe, J., *Hydrodyanmics around Cylindrical Structures*, World Scientific, 1997.

[5] Lam, K.M., Hu, J.C. & Liu, P., Vortex formation processes from an oscillating circular cylinder at high Keulegan-Carpenter numbers, *Phys. of Fluids.*, **22**, 2010, 015105-1-14.

[6] Westgate, Z.J., White, D.J. & Randolph, M.F., Field observations of as-laid pipeline embedment in carbonate sediments, *Géotechnique*, **62 (9)**, 2012, 787-798.

[7] Carpenter, L.H., On the Motion of Two Cylinders in an Ideal Fluid, *Jour. Res. Nat. Bur. Stands.*, **61 (2)**, 1958, 83-87.

[8] Stanier, S.A., Blaber, J., Take, W.A. & White, D.J., Improved image-based deformation measurement for geotechnical applications, *Can. Geotech. Jour.*, **53**, 2016, 1-13.